Measurement of the response of a gallium metal solar neutrino experiment to neutrinos from a ^{51}Cr source

J. N. Abdurashitov, V. N. Gavrin, S. V. Girin, V. V. Gorbachev, T. V. Ibragimova, A. V. Kalikhov, N. G. Khairnasov, T. V. Knodel, V. N. Kornoukhov,* I. N. Mirmov, A. A. Shikhin, E. P. Veretenkin, V. M. Vermul, V. E. Yants, and G. T. Zatsepin
Institute for Nuclear Research, Russian Academy of Sciences, 117312 Moscow, Russia

Yu. S. Khomyakov and A. V. Zvonarev†
Institute of Physics and Power Engineering, Obninsk, Russia

T. J. Bowles, J. S. Nico,‡ W. A. Teasdale, and D. L. Wark§
Los Alamos National Laboratory, Los Alamos, New Mexico 87545

M. L. Cherry
Louisiana State University, Baton Rouge, Louisiana 70803

V. N. Karaulov, V. L. Levitin, V. I. Maev, P. I. Nazarenko, V. S. Shkol'nik, and N. V. Skorikov
Mangyshlak Atomic Energy Complex, Aktau, Kazakhstan

B. T. Cleveland, T. Daily, R. Davis, Jr., K. Lande, C. K. Lee, and P. S. Wildenhain
University of Pennsylvania, Philadelphia, Pennsylvania 19104

S. R. Elliott and J. F. Wilkerson
University of Washington, Seattle, Washington 98195

(The SAGE Collaboration)

(Received 25 March 1998)

The neutrino capture rate measured by the Russian-American Gallium Experiment is well below that predicted by solar models. To check the response of this experiment to low-energy neutrinos, a 517 kCi source of ^{51}Cr was produced by irradiating 512.7 g of 92.4%-enriched ^{50}Cr in a high-flux fast neutron reactor. This source, which mainly emits monoenergetic 747-keV neutrinos, was placed at the center of a 13.1 ton target of liquid gallium and the cross section for the production of ^{71}Ge by the inverse beta decay reaction $^{71}\mathrm{Ga}(\nu_e, e^-)^{71}\mathrm{Ge}$ was measured to be $[5.55 \pm 0.60\ (\mathrm{stat}) \pm 0.32\ (\mathrm{syst})] \times 10^{-45}$ cm^2. The ratio of this cross section to the theoretical cross section of Bahcall for this reaction is $0.95 \pm 0.12\ (\mathrm{expt})^{+0.035}_{-0.027}$ (theor) and to the cross section of Haxton is 0.87 ± 0.11 (expt) ± 0.09 (theor). This good agreement between prediction and observation implies that the overall experimental efficiency is correctly determined and provides considerable evidence for the reliability of the solar neutrino measurement. [S0556-2813(99)03803-0]

PACS number(s): 26.65.+t, 13.15.+g, 95.85.Ry

I. INTRODUCTION

Gallium experiments are uniquely able to measure the principal component of the solar neutrino spectrum. This is because the low threshold of 233 keV [1] for inverse beta decay on the 40% abundant isotope ^{71}Ga is well below the end point energy of the neutrinos from proton-proton fusion, which are predicted by standard solar models to be about 90% of the total flux. The Russian-American Gallium Experiment (SAGE) has been measuring the capture rate of solar neutrinos with a target of gallium metal in the liquid state since January 1990. The measured capture rate [2,3] is $67 \pm 7\ (\mathrm{stat})^{+5}_{-6}\ (\mathrm{syst})$ SNU,[1] a value that is well below solar model predictions of 137^{+8}_{-7} SNU [4] and 125 ± 5 SNU [5]. In addition, the GALLEX Collaboration, which has been measuring the solar neutrino capture rate with an aqueous $GaCl_3$ target since 1991, observes a rate of $70 \pm 7^{+4}_{-5}$ SNU [6].

The other two operating solar neutrino experiments, the chlorine experiment [7] and the Kamiokande experiment [8], have significantly higher-energy thresholds, and thus are not able to see the neutrinos from *pp* fusion. When the results of

*Present address: Institute of Theoretical and Experimental Physics, 117259 Moscow, Russia.

†Deceased.

‡Present address: National Institute of Standards and Technology, Bldg. 235/A106, Gaithersburg, MD 20899.

§Present address: Department of Particle and Nuclear Physics, Oxford University, Keble Road, Oxford OX1 3RH, UK.

[1] 1 SNU corresponds to one neutrino capture per second in a target that contains 10^{36} atoms of the neutrino absorbing isotope.

these four solar neutrino experiments are considered together, a contradiction arises which cannot be accommodated by current solar models, but which can be explained if one assumes that neutrinos can transform from one species to another [9–15].

The gallium experiment, in common with other radiochemical solar neutrino experiments, relies on the ability to extract, purify, and count, all with well known efficiencies, a few atoms of a radioactive element that were produced by neutrino interactions inside many tons of the target material. In the case of 60 tons of Ga, this represents the removal of a few tens of atoms of ^{71}Ge from 5×10^{29} atoms of Ga. To measure the efficiency of extraction, about 700μg of stable Ge carrier is added to the Ga at the beginning of each exposure, but even after this addition, the separation factor of Ge from Ga is still 1 atom in 10^{11}. This impressively stringent requirement raises legitimate questions about how well the many efficiencies that are factored into the final result are known. It has been understood since the outset that a rigorous check of the entire operation of the detector (i.e., the chemical extraction efficiency, the counting efficiency, and the analysis technique) would be made if it is exposed to a known flux of low-energy neutrinos. In addition to verifying the operation of the detector, such a test also eliminates any significant concerns regarding the possibility that atoms of ^{71}Ge produced by inverse beta decay may be chemically bound to the gallium (so-called ''hot atom chemistry'') in a manner that yields a different extraction efficiency than that of the natural Ge carrier. In other words, it tests a fundamental assumption in radiochemical experiments that the extraction efficiency of atoms produced by neutrino interactions is the same as that of carrier atoms.

This article describes such a test, in which a portion of the SAGE gallium target was exposed to a known flux of ^{51}Cr neutrinos and the production rate of ^{71}Ge was measured. Similar tests have also been made by GALLEX [16].

Although a direct test with a well-characterized neutrino source lends significant credibility to the radiochemical technique, we note that numerous investigations have been undertaken during the SAGE experiment to ensure that the various efficiencies are as quoted [2]. The extraction efficiency has been determined by a variety of chemical and volumetric measurements that rely on the introduction and subsequent extraction of a known amount of the stable Ge carrier. A test was also carried out in which Ge carrier doped with a known number of ^{71}Ge atoms was added to 7 tons of Ga. Three standard extractions were performed, and it was demonstrated that the extraction efficiencies of the carrier and ^{71}Ge follow each other very closely.

Another experiment was performed to specifically test the possibility that atomic excitations might tie up ^{71}Ge in a chemical form from which it would not be efficiently extracted. There is a concern that this might occur in liquid gallium because the metastable Ga_2 molecule exists with a binding energy of $\sim$1.6 eV. In this experiment the radioactive isotopes ^{70}Ga and ^{72}Ga were produced in liquid gallium by neutron irradiation. These isotopes quickly beta decay to ^{70}Ge and ^{72}Ge. The Ge isotopes were extracted from the Ga using our standard procedure and their number was measured by mass spectrometry. The results were consistent with the number expected to be produced based on the known neutron flux and capture cross section, thus suggesting that chemical traps are not present. This experiment is not conclusive, however, because the maximal energy imparted to the ^{70}Ge nucleus following beta decay of ^{70}Ga is 32 eV, somewhat higher than the maximal energy of 20 eV received by the ^{71}Ge nucleus following capture of a 747-keV neutrino from ^{51}Cr decay (and considerably higher than the maximum nuclear recoil energy of 6.1 eV after capture of a 420-keV neutrino from proton-proton fusion).

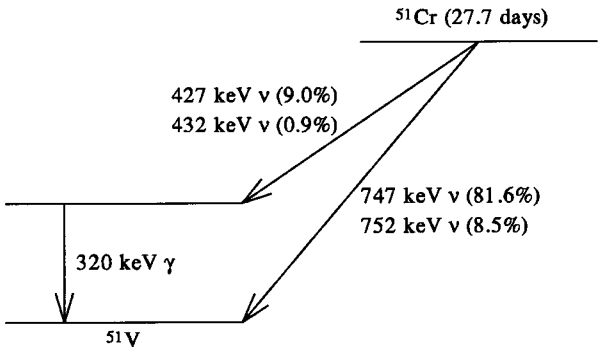

FIG. 1. Decay scheme of ^{51}Cr to ^{51}V through electron capture.

Further evidence that the extraction efficiency was well understood came from monitoring the initial removal from the Ga of cosmogenically produced ^{68}Ge. This nuclide was generated in the Ga as it resided on the surface exposed to cosmic rays. When the Ga was brought underground, the reduction in the ^{68}Ge content in the initial extractions was the same as for the Ge carrier. These numerous checks and auxiliary measurements have been a source of confidence in our methodology, yet it is clear that a test with an artificial neutrino source of known activity provides the most compelling validation of radiochemical procedures.

This article is an elaboration of work that previously appeared in Ref. [17]. The experimental changes since the previous Letter are some minor refinements in the selection of candidate ^{71}Ge events and in the treatment of systematic errors; recent cross section calculations are also included. The central experimental result given here is almost identical to what was reported earlier.

II. ^{51}Cr SOURCE

A. Choice of chromium

A number of *K*-capture isotopes that can be produced by neutron irradiation in a high-flux reactor, ^{51}Cr, ^{65}Zn, and ^{37}Ar, have been suggested [18–21] as sources that can be used to check the response of solar neutrino detectors. The isotope ^{51}Cr emits neutrinos with energy closest to the *pp* neutrinos, the solar neutrino component to which gallium is most sensitive, and thus is the best choice for the gallium experiments.

The decay of ^{51}Cr is by electron capture, $^{51}\mathrm{Cr}+e^-\rightarrow{}^{51}\mathrm{V}+\nu_e$, with a half-life of 27.7 d. The decay scheme is illustrated in Fig. 1. There is a 90.12% branch [22] that decays directly to the ground state of ^{51}V and a 9.88% branch which decays to the first excited state of ^{51}V, which promptly decays with the emission of a 320-keV gamma ray to the ground state. Taking into account the atomic levels to which transitions can occur, the neutrino energies are 752

TABLE I. Isotopic composition of natural Cr and of the enriched Cr in the source.

Isotope	Abundance (%)	
	Natural	Enriched
50	4.35	92.4±0.5
52	83.79	7.6±0.4
53	9.50	<0.5
54	2.36	<0.2

keV (9%), 747 keV (81%), 432 keV (1%), and 427 keV (9%).

The intensity of the ^{51}Cr source must be high enough that the production rate in the gallium target is significantly greater than the solar neutrino capture rate. The source activity is thus required to be near to 1 MCi, far surpassing the activity of most sources produced at reactors. Because ^{50}Cr has only a 4.35% natural abundance, it is impossible to produce the necessary activity of ^{51}Cr by irradiation of natural Cr in any presently existing nuclear reactor. The required activity can only be attained by irradiation of enriched ^{50}Cr, as shown in Ref. [23] and additionally considered in Ref. [24]. Besides decreasing the irradiated mass to a value that can be acceptably placed in a reactor, the use of enriched Cr reduces the self-shielding during irradiation and reduces the neutron competition from ^{53}Cr, whose capture cross section for thermal neutrons is very high.

The chromium used in our experiment was enriched to 92.4% in ^{50}Cr. The isotopic composition is given in Table I. The advantage of this high enrichment was that it yielded a source of great specific activity (more than 1 kCi/g) and small physical size, thus giving a very high neutrino capture rate.

B. Cr preparation

Enriched chromium was produced by the Kurchatov Institute by gas centrifugation of chromium oxyfluoride, CrO_2F_2 [25,26]. The highly corrosive CrO_2F_2 was then hydrolyzed to chromium oxide, Cr_2O_3. To obtain an extremely compact source, the chromium oxide was then reduced to metallic chromium. This reduction was done by heating a cold-pressed mixture of chromium oxide and high-purity graphite in a hydrogen atmosphere; the resulting product was melted in an Al_2O_3 crucible to remove gaseous impurities. The Cr ingots were then crushed into pieces of 1–3 mm size and the chromium was treated with hydrogen at 1200 °C for 24 hours to remove residual oxygen and nitrogen.

For the reactor irradiation the metallic Cr was extruded into the form of rods, 45 mm long by 7 mm in diameter. Cr chips were placed into a molybdenum-lined steel shell under modest pressure at room temperature and the shell was electron beam welded in vacuum (10^{-6} torr). This shell with the enclosed chromium was subjected to very high pressure at 1100 °C for 30 seconds and then extruded at 1000 °C such that the length of the Cr was increased by a factor of 7. The steel shell was then dissolved in nitric acid and chromium rods of the desired size were produced by machining and spark cutting. Finally, the rods were recrystallized at 1000 °C. The measured density (taking into account the Cr isotopic composition), grain size, and hardness of the resulting rods were very close to those of pure defectless metallic chromium. Table II gives the properties of the 50 rods that were prepared. Their microstructure was essentially identical to that of pure metallic Cr.

TABLE II. Properties of the Cr rods prepared for irradiation.

Characteristic	Lot 1	Lot 2	Lot 3
Number of rods	21	21	8
Total mass of Cr (g)	245.8	244.9	93.43
Hardness (kg/mm^2)	138	134	152
Grain size (μm)	18	24	23
Density (g/cm^3)	6.93	6.96	6.96

C. Cr irradiation and source assembly

The Cr was irradiated at the BN-350 fast breeder nuclear reactor at the atomic power station in Aktau, Kazakhstan. This reactor was designed for simultaneous power and secondary nuclear fuel production. Other similar reactors are BN-600 in Russia, Phenix and Super Phenix in France, and MONJU in Japan. BN-350 has a core of highly enriched uranium without a moderator and a blanket of unenriched uranium; liquid Na is used as a coolant. This construction gives a high flux of fast neutrons [to 5×10^{15}/(cm^2 s)] at nominal power, which is advantageous for making intense sources [27].

The cross section for capture of fast neutrons by ^{50}Cr is less than 0.1 b, much too low to reach the desired specific activity of ^{51}Cr. Therefore a unique irradiation assembly (IA) was developed, which could be placed in the BN-350 core as a replacement fuel assembly (see Fig. 2 and Fig. 3). Most of the volume of the IA consisted of a zirconium hydride moderator around a central stainless steel tube that contained the ^{50}Cr metal rods. This gave a high flux of low-energy neutrons in the vicinity of the ^{50}Cr, and as a result, a much increased average capture cross section ($\sim$4 b). To prevent leakage of these low-energy neutrons from the IA, which could increase the power release in neighboring fuel assemblies, the moderator was surrounded by absorbing elements made of europium oxide. Finally, the presence of the IA results in a negative reactivity effect. To compensate for this the standard configuration of the reactor core was altered by replacing a few assemblies with ones of higher fuel enrichment and by installing a few additional fuel assemblies.

Calculations showed that by using two irradiation assemblies we would expect to produce a source whose activity at the end of irradiation was between 0.5 and 0.8 MCi, depending on reactor power and the position in the reactor core where the IA was irradiated. The final physical characteristics of the IA were measured in a low-power experiment, which was carried out in the BN-350 reactor before the full-scale irradiation. This experiment showed safe irradiation of the IA but gave less ^{51}Cr activity than anticipated. To compensate for this reduced activity it was decided to increase the reactor power near the end of irradiation. The IA's were installed on 4 September 1994 with the reactor power set at its usual level of 520 MW. Irradiation continued until 2 December, at which time the power was increased to 620 MW,

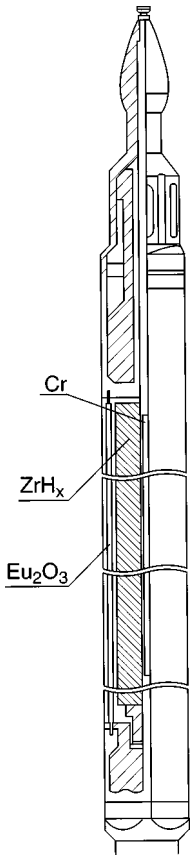

FIG. 2. Irradiation assembly (IA).

so as to increase the final ^{51}Cr activity. The IA's were removed from the reactor on 18 December 1994. Using remote manipulators inside a hot cell, all 46 irradiated Cr rods were removed from the IA's and 44 of them, whose total mass before irradiation was 512.7 g, were placed into holes in a tungsten holder. This holder was then put into a stainless steel casing and the assembly was welded shut and leak checked in a helium atmosphere. This source assembly was placed in a specially constructed tungsten radiation shield with 18 mm wall thickness, which had an outer stainless steel casing of 80 mm diameter by 140 mm height. The outer stainless shell was also welded shut and leak checked. A cutaway view of the overall source assembly is shown in Fig. 4. This source was placed into a shipping cask, flown to the Mineralnye Vody airport in southern Russia, and then transported by truck to the Baksan Neutrino Observatory where the ^{51}Cr irradiations of the gallium were carried out.

D. Source impurities

There exist a large number of chemical elements that, upon irradiation, produce long-lived gamma-emitting isotopes. The presence of these gamma emitters in the source must be strictly controlled because they increase the size of the source shield necessary for personnel protection and thus decrease the effective neutrino path length in the gallium target, and they add heat to the source and thus confuse the calorimetric measurement of source activity which will be described below. Because of their high capture cross section for thermal neutrons, even minute quantities of some elements cannot be tolerated.

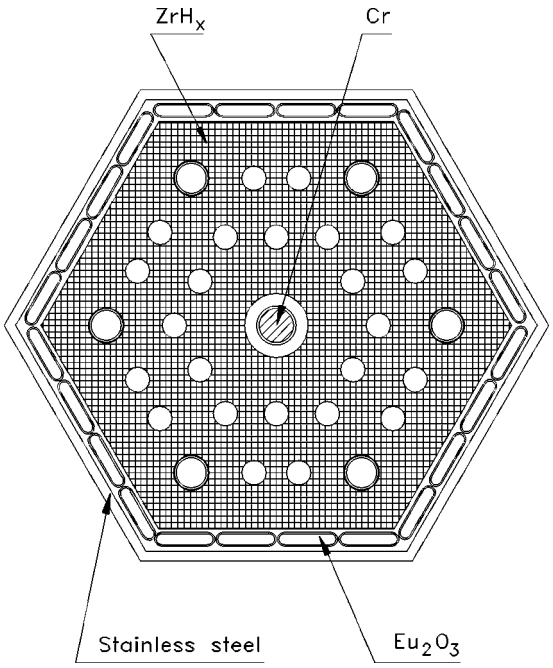

FIG. 3. Cross section of irradiation assembly (IA). The open circles are cooling channels for liquid Na.

As a consequence, special care was taken in all the stages of chemical processing to minimize contamination of the Cr. To be confident that the final impurity content of the Cr rods was satisfactory, each rod was chemically analyzed before irradiation by ICP-mass spectrometry with laser ablation and by spark mass spectrometry. The concentrations of the most relevant impurities are given in Table III, together with the expected and measured activities after irradiation. The dose rate at the side surface of the source was 1.7 Sv/h at the beginning of the first exposure (26 December 1994) and only $\sim$2% of this was due to impurities (mostly ^{46}Sc). At the end of the last exposure (23 May 1995), the dose rate had de-

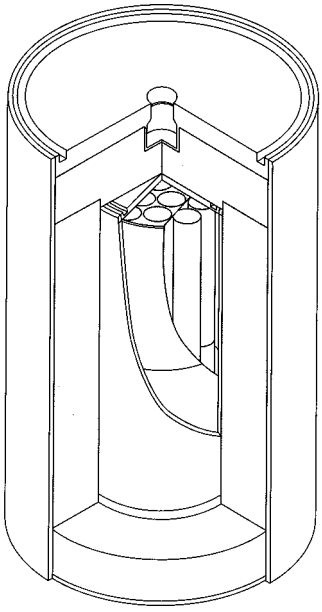

FIG. 4. Cutaway drawing of the source. The Cr rods were placed within the inner cylinders.

TABLE III. Measured impurities in the Cr rods prior to activation and the predicted resulting activities at the reference time (18:00 on 26 Dec. 1994). These are compared to the measured activities.

Impurity	Measured Content (ppm)	Nuclide	Half-life	Activity (mCi)	
				Expected	Measured
Fe	50.0	^{59}Fe	44.5 d	9	24±3
W	25.0	^{187}W	23.9 h	23	negligible
Cu	15.0	^{64}Cu	12.7 h	<0.1	negligible
Ga	5.7	^{72}Ga	14.1 h	<0.1	negligible
Na	3.3	^{24}Na	15.0 h	<0.1	negligible
Zn	3.3	^{65}Zn	244. d	17	negligible
Ta	3.0	^{182}Ta	115. d	1930	38±5
Co	1.0	^{60}Co	5.3 y	81	65±15
Sc	0.9	^{46}Sc	83.3 d	860	1400±100
As	0.6	^{76}As	26.3 h	2	negligible
Sb	<0.1	^{124}Sb	60.2 d	<13	negligible
La	<0.1	^{140}La	40.3 h	<0.4	negligible

creased to 0.05 Sv/h, with an increase in the fraction due to impurities to ~25%.

Figure 5 shows a gamma spectrum of the source taken shortly after the start of the first Ga irradiation. The 320-keV gamma ray from ^{51}Cr decay was attenuated by a large factor by the tungsten shield, but still was the most intense line in the spectrum. The higher energy lines of ^{46}Sc, ^{59}Fe, ^{60}Co, and ^{182}Ta had much smaller attenuations and thus produced lines, even though their activity was much lower than that of ^{51}Cr. Limits on the level of contamination activity can be inferred from this spectrum and are summarized in Table IV. The 1.5 Ci activity of ^{46}Sc was the largest single contribution and the total activity of all contaminants was estimated to be less than 2 Ci at this time.

Table III compares the values of activities expected from the preirradiation impurity determinations and those measured afterwards. The only significant difference was for Ta, which was because the mass-spectrometric analysis preferentially sampled the surface of the Cr rods and not the bulk material. The apparently high concentration of Ta in the Cr resulted from surface contamination by the tungsten carbide tool used to machine the rods to the desired diameter.

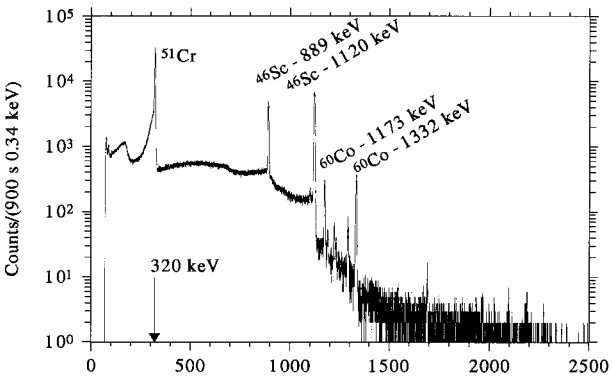

FIG. 5. Unshielded Ge detector spectrum of the gamma rays emitted by the Cr source taken on 7 January 1995 at 10:40. Gamma lines are labeled by the isotope of origin. Other contaminants whose lines are not labeled include ^{59}Fe, ^{182}Ta, and ^{124}Sb.

III. EXTRACTION SCHEDULE

The 55 tons of Ga that SAGE uses for solar neutrino measurements is contained in eight chemical reactors with approximately 7 tons in each. Figure 6 shows the layout of the ten reactors in the experimental area and gives their numerical identification assignments. In normal solar neutrino operation Ga is contained in reactors 2–5 and 7–10. All reactors except No. 6 are equipped with the necessary mechanical equipment for the extraction process. Reactor 6 was modified for the Cr exposures by removing its stirring mechanism and replacing it with a reentrant Zr tube on its axis which extended to the reactor center. This modification increased the capacity of reactor No. 6 to 13 tons of Ga. To begin each irradiation, a specially designed remote handling system was used (Fig. 7) to place the ^{51}Cr source inside this reentrant tube at the reactor center. At the end of each irradiation, the source was moved to an adjacent calorimeter for activity measurement, and the gallium was pumped back to the two reactors where it was stored during solar neutrino runs. The ^{71}Ge was then extracted with the usual chemical procedures [28,29].

The source arrived at Mineralnye Vody on 20 December 1994. Because of a delay in customs approval, it was not delivered to the laboratory in Baksan until 26 December 1994. The initial installation of the source into the Ga was at 18:00 on 26 December. We normalize all our results to this time. Eight extractions were conducted between 2 January and 24 May 1995. See Table V for a summary of the extraction dates. The lengths of the exposure periods for the first five measurements were chosen so each would have approximately equal statistical uncertainty. After these initial extractions, the Cr source had decayed to the point where this was no longer possible and the final three extractions were done at approximately monthly intervals, the same schedule as for solar neutrino extractions.

The Cr experiment used reactors 6–10, shown in Fig. 6. To start the first exposure Ga was pumped from reactors 9 and 10 to irradiation reactor 6 and then the ^{51}Cr source was inserted to the center of this reactor. At the end of exposure 1 the source was moved to the calorimeter and the Ga was

TABLE IV. Measured nuclide impurities in the ^{51}Cr source and their contribution to the source activity measurement at the reference time (18:00 on 26 Dec. 1994). The power estimation assumes that all the available energy is deposited in the calorimeter. A row with the data for the ^{51}Cr is included for comparison. The conversion constant 36.671 keV/decay was used in estimating the power for the Cr.

Isotope	Q value (MeV)	Measured activity (Ci)	Estimated power (W)	Equivalent ^{51}Cr activity (kCi)
^{46}Sc	2.37	1.400±0.1	0.0200	0.092
^{60}Co	2.82	0.065±0.015	0.0011	0.005
^{182}Ta	1.81	0.038±0.005	0.0004	0.002
^{59}Fe	1.56	0.024±0.003	0.0002	0.001
Impurity total			0.0217	0.1
^{51}Cr	0.32	516600±6000	112.3000	516.6

pumped to reactors 9 and 10 for extraction. Immediately following this extraction, the Ga was pumped to reactor 6 from reactors 9 and 10 and the source was again placed at the center of reactor 6 to begin exposure 2. Upon completion of exposure 2, the Ga was once again pumped to reactors 9 and 10. This time, however, two extractions were done–Nos. 2 and 2-2. Meanwhile, 13.134 tons of Ga from reactors 7 and 8 was pumped to reactor 6 to begin exposure 3. This pattern of exposure and extraction was repeated for a total of eight exposures. For exposures 1, 2, 5, and 6 the Ga was extracted in reactors 9 and 10. For exposures 3, 4, 7, and 8 the Ga was extracted in reactors 7 and 8. Second extractions followed exposures 2, 4, 6, and 7.

This extraction procedure differed somewhat from that used for the solar neutrino experiment because there was the additional step of the Ga transfer from two reactors to the irradiation vessel and back. Although there is no obvious reason why this should introduce a change in extraction efficiency, a number of tests were conducted to be confident that this efficiency was not altered by the Ga transfer. Prior to the ^{51}Cr source exposure, nine solar neutrino extractions were done from one or two reactors using all steps of the above procedure including the Ga transfer. The measured production rate in these experiments was 92 SNU with a 68% confidence range from 53 SNU to 143 SNU. This capture rate was entirely consistent with that from solar neutrinos and no change was observed in the counter background.

IV. SOURCE ACTIVITY DETERMINATION

A. Source activity from calorimetry

The decay of ^{51}Cr deposits energy in the form of heat in its surroundings. Since all but 1 part in 10^5 of the ^{51}Cr radiation was absorbed in the source, the source activity could be determined by measuring its heat with a calorimeter. Table VI gives a summary of the energy released in ^{51}Cr decay neglecting the energy lost to neutrinos. The average

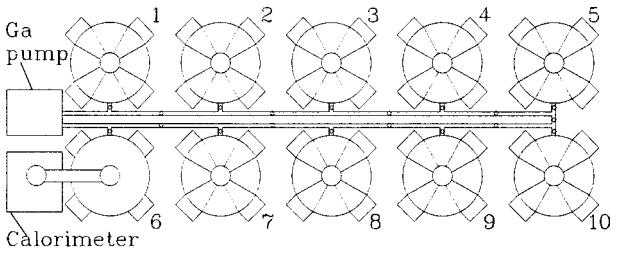

FIG. 6. Plan view of the laboratory showing the ten chemical reactors, irradiation reactor 6 with the adjacent calorimeter, and the Ga pump for transferring Ga between reactors.

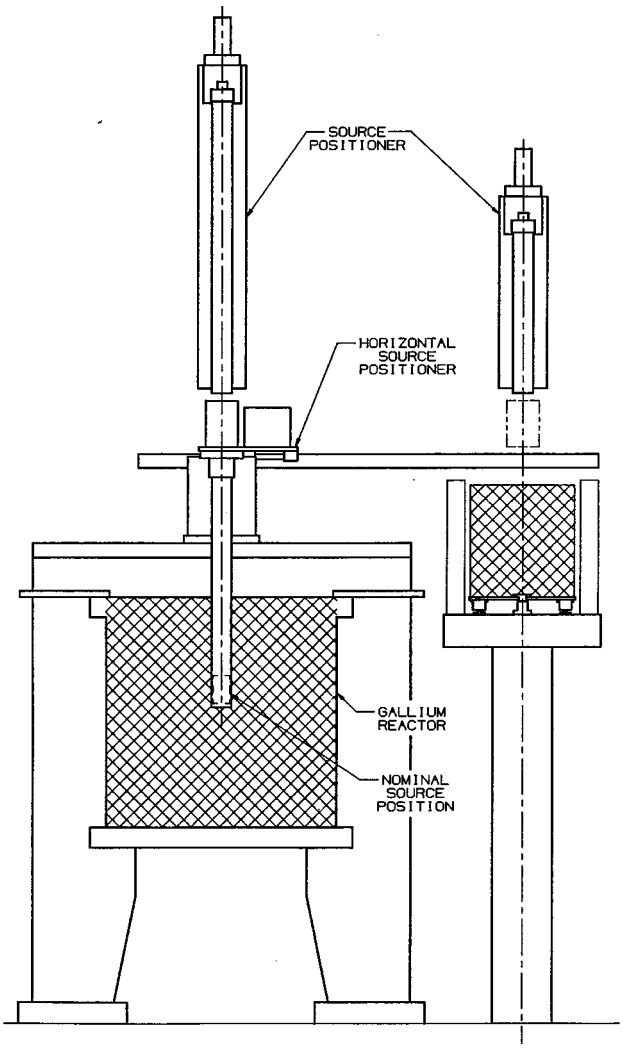

FIG. 7. Schematic drawing of the remote handling system which moved the ^{51}Cr source from the gallium-containing reactor to the adjacent calorimeter.

TABLE V. Extraction schedule and related parameters. The times of exposure are given in days of year 1995.

Extraction name	Extraction date (1995)	Source exposure		Source activity (kCi)		Solar neutrino exposure		Mass Ga (tons)	Extraction efficiency	
		Begin	End	Begin	End	Begin	End		from Ga	into GeH_4
Cr 1	2 Jan.	−4.25	1.86	516.6	443.4	−10.58	2.05	13.123	0.85	0.82
Cr 2	9 Jan.	2.60	9.33	435.2	367.8	1.55	9.50	13.108	0.88	0.84
Cr 2-2	11 Jan.	2.60	9.33	435.2	367.8	9.50	11.46	13.094	0.85	0.71
Cr 3	18 Jan.	9.65	18.32	364.9	293.7	5.45	18.50	13.134	0.86	0.80
Cr 4	3 Feb.	19.04	34.32	288.5	196.8	18.50	34.49	13.119	0.89	0.85
Cr 4-2	5 Feb.	19.04	34.32	288.5	196.8	34.49	36.48	13.106	0.86	0.80
Cr 5	1 Mar.	34.84	60.46	194.3	102.3	11.46	60.63	13.081	0.90	0.83
Cr 6	24 Mar.	61.33	83.40	100.1	57.6	60.63	83.60	13.067	0.86	0.82
Cr 6-2	26 Mar.	61.33	83.40	100.1	57.6	83.60	85.45	13.054	0.85	0.79
Cr 7	23 Apr.	83.99	113.33	56.8	27.3	36.48	113.52	13.090	0.84	0.81
Cr 7-2	26 Apr.	83.99	113.33	56.8	27.3	113.52	116.46	13.077	0.87	0.72
Cr 8	24 May	118.83	143.86	23.8	12.7	116.46	144.54	13.063	0.92	0.82

energy released which can be detected as heat is 36.67 ± 0.20 keV/decay where the uncertainties have been added in quadrature.

The special calorimeter shown in Fig. 8 was built [30] to measure the heating power from the ^{51}Cr source. It consisted of two identical calorimetric transducers located side by side. The internal section of each transducer, into which the ^{51}Cr source was placed, was a copper cup 95 mm in diameter and 150 mm high, with a wall thickness of 5 mm. The copper cup was inside the air cavity of a large 68-kg copper block. A thermopile consisting of 120 Chromel-Alumel thermocouples connected in series was placed between the cup and the internal wall of the copper block. Thermocouple hot junctions were distributed evenly over the cup surface; the cold junctions were fixed to the internal surface of the copper block. The voltage produced by the thermopile was thus proportional to the temperature difference between the cup and its copper block. The heat produced by the source was quite large; to improve the heat exchange eight copper plates were placed between the cup and the copper block. The power of the source warmed the cup and provided heat that was transferred to the copper block. This can be expressed as

$$P = c\frac{dT_s}{dt} + K\Delta T, \tag{1}$$

where P is the heat power of the source (W), c is the heat capacity of the source and the cup (J/°C), T_s is the temperature of the source and cup (°C), t is the time (s), K is the heat-transfer coefficient [J/(°C s)], and ΔT is the temperature difference between the cup and the copper block (°C). The first term in Eq. (1) represents the heating of the source-cup system; the second term describes the transfer of heat to the copper block.

To understand the operation of the calorimeter, consider a typical measurement. When the source was first put into the cup, $\Delta T = 0$; so all heat from the source served only to warm the cup. Then, as the temperature of the cup increased, heat began to be transferred to the copper block and the heating rate of the cup containing the source decreased. When thermal equilibrium was reached, which required approximately 6 h, the cup-source system was at a constant temperature and all heat produced by the source was transferred to the copper block. In this condition the signal from the thermopile was constant, and the source thermal power, by Eq. (1), was determined only by the temperature difference ΔT and the heat-transfer coefficient K.

The heat-transfer coefficient K was determined using electroheaters made from steel or aluminum whose outside dimensions coincided exactly with the outside dimensions of the source. The heater power was varied by controlling the

TABLE VI. Summary of the input data to the power generated during the decay of ^{51}Cr. The value for the M-shell fraction is deduced from the average of the M/L ratios for the electron capture isotopes ^{37}Ar and ^{55}Fe.

Type of radiation	Energy (keV)	Fraction of ^{51}Cr decays	Energy released per ^{51}Cr decay (keV)
Gamma	320.0852(9) [22,31]	0.0988(5) [22]	31.624(160)
K capture	5.465 [43]	0.895(5) [44]	4.891(25)
L capture	0.628 [43]	0.0925(50) [44]	0.058(2)
M capture	0.067 [43]	0.0125 (calc)	0.001 (small)
Int. bremss.	751 (end point)	$3.8\times10^{-4}\times0.902$ ($\pm\sim10\%$)	0.096(10) [34]
Int. bremss.	430 (end point)	$1.2\times10^{-4}\times0.0983$ ($\pm\sim10\%$)	0.001 (small)
Total			36.671(197)

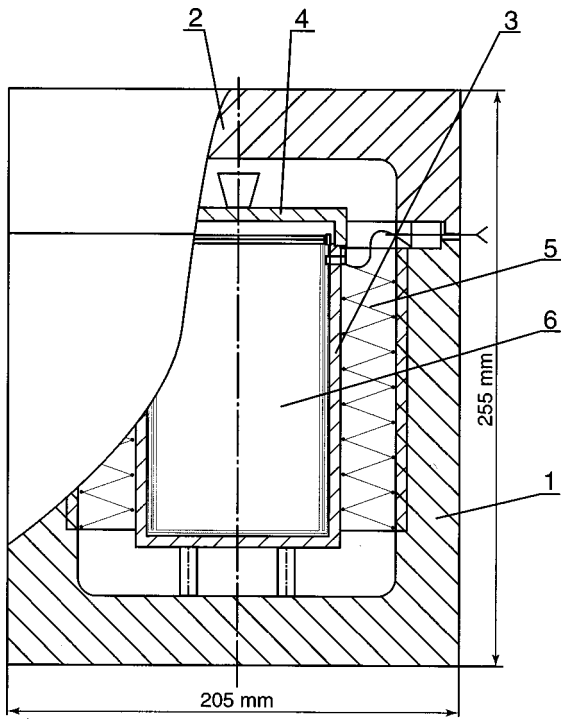

FIG. 8. Schematic drawing of the calorimeter. Individual parts are (1) copper block, (2) lid of copper block, (3) copper cup, (4) lid of copper cup, (5) thermopile, and (6) source or electroheater.

current to an internal Nichrome or constantan winding. Each heater was used for calibration up to its maximum power.

The calibration curve of the thermistor reading as a function of heater power in watts is shown in Fig. 9. The uncertainty associated with each measurement was approximately $\pm 2\%$. A fit to the calibration curve with a second-order polynomial gave the result

$$P = 0.43(14) + 0.2418(41)V + 0.000\,159(16)V^2, \quad (2)$$

where P is the power in watts and V is the thermistor reading in mV. The numbers in parentheses represent the uncertainties in the final digits of each parameter. With each measurement weighted by the 2% uncertainty, χ^2 for the fit was 36.9 for 35 data values.

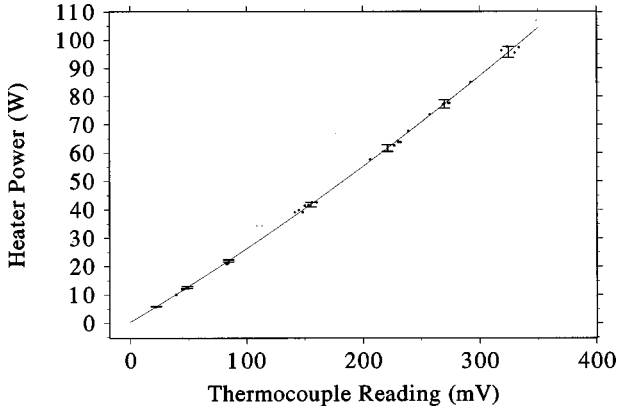

FIG. 9. Calibration curve of the calorimeter. The thermocouple readings and the inferred power for the seven measurements of the Cr source are also indicated.

TABLE VII. Source power measurements with the calorimeter.

Days after 18:00 on 26 Dec. 1994	Thermocouple voltage (mV)	Deduced power (W)	Power on 26 Dec. 1994 (W)
6.62	324.8	95.7±1.9	112.9±2.2
13.90	269.9	77.2±1.5	109.3±2.2
23.08	221.2	61.6±1.2	109.8±2.2
39.08	155.36	41.8±0.8	111.1±2.2
66.21	84.46	22.0±0.4	115.1±2.3
88.17	48.88	12.6±0.3	114.5±2.3
118.17	22.20	5.9±0.1	113.0±2.3

The heat produced by the ^{51}Cr source was measured between extractions for a total of seven measurements. The results of these measurements are shown numerically in Table VII and graphically in Fig. 10. The uncertainty in each measurement is only that propagated from the calibration curve. Each value is normalized to the activity on 26 December at 18:00 taking into account the decay of the ^{51}Cr. A weighted average of these seven power measurements gives a value on 26 December at 18:00 of 112.3±0.8 W (Fig. 10). χ^2 for this average is 6.0. As a test, we performed this same fit, allowing the parameter associated with the ^{51}Cr half-life to vary. The best fit half-life was determined to be 28.03 ±0.23 days, in reasonable agreement with the known value of 27.702±0.004 days [22,31].

The decay of ^{51}Cr gives an average energy release of 36.67±0.20 keV/decay. Using 1.6022×10^{-19} (W s)/eV and 3.7×10^{10} decays/(Ci s), this implies a conversion factor of

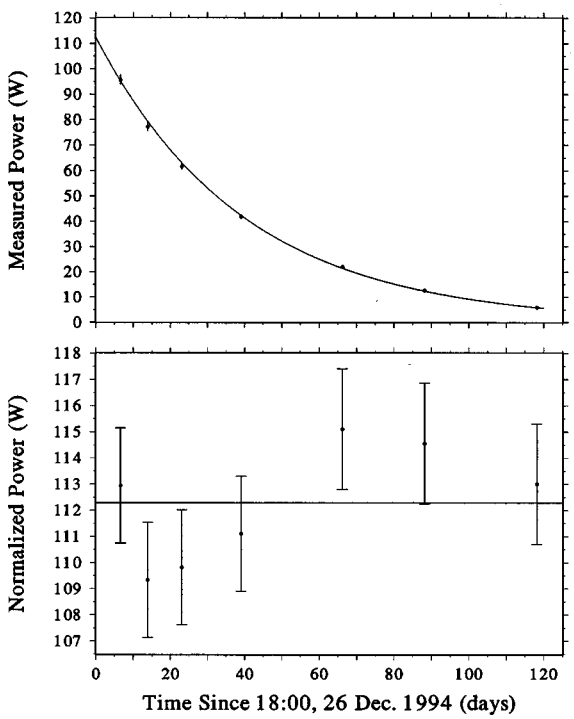

FIG. 10. The seven individual source activity measurements. The line is a weighted fit to the data points with an exponential function whose half-life is that of ^{51}Cr. In the lower panel the power is normalized to 18:00 on 26 December 1994.

TABLE VIII. Summary of the uncertainties associated with the source activity as deduced from the calorimetry data. In the total, the uncertainty due to contamination is taken to be the larger of the two extremes. All uncertainties are symmetric.

Origin of uncertainty	Uncertainty	
	Percentage	Magnitude (kCi)
Statistics (112.3±0.8 watts)	0.8	3.9
Calorimeter equilibration	0.6	3.1
Power to activity conversion (4.600±0.025 kCi/W)	0.54	2.8
^{51}Cr half-life (27.702±0.004 days)	0.2	1.0
Contamination (26 December 1994)	0.02	0.10
Contamination (24 April 1994)	0.14	0.72
Total uncertainty (added in quadrature)	1.2	6.0

4.600±0.025 kCi ^{51}Cr/W. The ^{51}Cr activity at the time it was first placed in the reactor containing Ga was thus 516.6 ±3.7 kCi, where the uncertainty is entirely statistical.

Several systematic uncertainties are associated with this source activity determination. Before taking a thermocouple measurement we waited for 12 h to be sure that the source (or electroheater) and the copper block in the calorimeter were in thermal equilibrium. It is estimated that the uncertainty due to different stabilization times between the source and the calibration heaters can be no more then 0.6% or 3.1 kCi.

The 0.54% uncertainty in the energy released per ^{51}Cr decay leads directly to an uncertainty of ±2.8 kCi in the source activity. We should note that the value we use for the energy release differs slightly from the value of 36.510 ±0.161 keV/decay used in Ref. [32]. There are two primary differences between these calculations: First, Ref. [32] used a branching ratio to the 320-keV level of 0.0986 [33], whereas we chose to use 0.0988 [22]. Second, Ref. [32] ignored the contribution of internal bremsstralung, which contributes approximately 96 eV/decay to the average [34], whereas we have included it here.

The half-life of Cr is known to 0.02%. To estimate how large an uncertainty this introduced in our source activity estimate, we repeated the fit to the Cr decay curve using a value for the half-life which differed from the known value by one standard deviation. This changed the power determination by 0.2% or 1.0 kCi and we take that as an estimate of the related uncertainty.

Radioactive impurities in the source can also give rise to heat which would be incorrectly attributed to ^{51}Cr. The impurity content of the source was considered above in Sec. II D, and the contribution of each impurity to the source power is given in Table IV. The effective Cr activity from all impurities was only 100 Ci at the reference time of 18:00 on 26 December 1994, which is a completely negligible 0.02% uncertainty. Because the half-life of the impurities was longer than that of Cr, the fractional size of this error increased with time. For the final calorimeter measurement on 24 April 1995, the fraction had risen to 0.14%.

Other possible contributions to the systematic uncertainty in the calorimetric determination of the source activity have been considered, such as the escape of some of the 320-keV gamma rays of ^{51}Cr from the source. All such contributions were shown to be negligible. Table VIII summarizes the various components of the source activity uncertainty that were described above. Adding the statistical and systematic components in quadrature gives the final value of 516.6± 6.0 kCi at the reference time.

The following subsections describe other independent methods used to measure the source activity. The calorimeter technique is the most precise and we use its result; the other methods add confidence in the calorimetric determination.

B. Source activity from direct counting

This section describes an independent determination of the source activity that used a Ge(Li) detector to measure the 320-keV gamma rays emitted by ^{51}Cr. Because of the high initial activity of the source, these measurements could only be carried out after the gallium exposures at the Baksan Neutrino Observatory had finished and the source had been returned to Aktau. At that time the ^{51}Cr activity had decreased by a factor of more than 1000.

The procedure for these measurements consisted of two steps: first, the relative activity of all 44 Cr rods was measured, and second, the absolute activity of a single monitor rod was determined. For the first step, two collimators were installed in the hot chamber of BN-350. A chromium rod was placed in a special transit in front of the slit of the first collimator. The transit moved in a vertical direction using a manipulator of the hot chamber and contained a motor which rotated the rod during measurement. The position of the Cr rod in relation to the collimator slit was controlled by electronic readout of the manipulator and by visual observation. Gamma rays passed through the slit of the second collimator and were counted by a Ge(Li) detector outside the hot cell. The activity of each rod was measured at three points along its length and the angular distribution was averaged because of the rotation of the rod. This system provided the average value of the activity of all Cr rods. The uncertainty in the relative activity of one rod was 1% and was determined by statistics, background, and the stability of the measurement geometry. The uncertainty in the sum of the relative activities of all rods was added in quadrature, resulting in an uncertainty of 0.3%.

The second step was to measure the absolute activity of the monitor rod. This rod was completely dissolved in HCl

acid. A small portion of this solution was diluted to prepare samples and their activity was measured. The uncertainty in activity from differences in sampling procedure was 3%; there was also a 1% error in volume because of the successive dilutions.

The standard deviation of a set of measurements of the count rate in the ^{51}Cr photopeak had an uncertainty of 1.2% due to statistics, background, and a dead time correction factor. The uncertainty in the efficiency of the detector was 3%. The ratio of the mass of the monitor rod to the mass of all rods in the source had a 1% uncertainty. The quadratic sum of all these uncertainties was 4.7%. The final result of this method of source activity measurement is 510 ± 24 kCi at our reference time (18:00 on 26 December 1994).

C. Source activity from reactor physics

The source activity can be determined, in principle, by direct neutron transport calculations using the geometry of the reactor and the irradiation assemblies. Such a calculation has many difficulties which limit its precision. Based on test results from the experimental reactor at Obninsk and irradiation of a small mass of ^{50}Cr in the reactor at Aktau, the calculated activity was 554 ± 55 kCi at our reference time, in agreement with the calorimeter measurement.

V. COUNTING OF ^{71}Ge

The number of ^{71}Ge atoms extracted from gallium was determined by the same procedure as used for solar neutrino measurements. Very briefly, the extracted Ge was synthesized into the counting gas GeH_4, mixed with Xe, and inserted into a very-low-background proportional counter. All pulses from this counter were then recorded for about the next 6 months. The counter body was made from synthetic quartz and cathode from ultrapure Fe; the volume was about 0.75 cm^3. To detect and suppress background, the counter was placed in the well of a large NaI detector, which was in turn contained within a massive Cu, W, Pb, and Fe passive shield. The parameters of counting are given in Table IX.

The data-recording system made hardware measurements of the pulse energy, ADP (a parameter inversely proportional to the pulse rise time during the first few ns), energy and time of any NaI events that occurred within -8 ms to $+8$ ms of the counter pulse, and event time. In addition, all the first extractions were measured in a counting system that digitized the pulse waveform for 800 ns after pulse onset.

^{71}Ge decays by electron capture with an 11.4-day half life and emits Auger electrons and x rays whose sum energy is usually either 10.4 keV (the *K* peak) or 1.2 keV (the *L* peak). The radial extent of these low-energy electrons in the counter is very short, producing a pulse waveform with a fast rise time. Background events, such as a minimum ionizing particle that traverses the counter, may deposit a similar amount of energy in the counter gas, but will usually have longer radial extent and hence slower rise time. Measurement of the rise time thus gives a very powerful suppression of background. For all first extractions the rise time was determined by fitting the digitized waveform to an analytical formula [35] that describes the pulse shape in terms of the radial extent of the trajectory in the counter.

The counters had a hole in the cathode near the center of the active volume with a thin section in the quartz envelope so the gas filling could be directly irradiated with the 5.9-keV x rays from ^{55}Fe. Counters were calibrated with ^{55}Fe just before the start of counting, about 3 days later, 1 week later, and then at 2–3-week intervals until counting ended. At least four ^{55}Fe calibrations were made for each run during the first month of counting, while the ^{71}Ge was decaying. For all eight first extractions the average change in the ^{55}Fe peak position during this time was 2.4%. They were also calibrated with ^{109}Cd which fluoresced the Fe cathode and made 6.4-keV x rays throughout the counter volume. For these ^{109}Cd calibrations, the source was positioned so that it did not see the side hole in the cathode; the peak position was thus representative of the response of the entire counter. By comparing the predicted position of the 6.4-keV peak based on the ^{55}Fe calibration with the actual position in the ^{109}Cd calibration, a correction factor was derived that modified the energy scale from the ^{55}Fe calibration to account for any polymerization that might be present on the anode wire in the vicinity of the side hole. For the eight first extractions this correction averaged 4.5% with a range from 0% to 11%.

TABLE IX. Counting parameters. Δ is the exponentially weighted live time after all time cuts have been applied. The second extractions were not counted in an electronics system with a digitizer so *L*-peak analysis could not be performed. There are no entries for Cr 2-2 as the counter failed and for Cr 7-2 as the sample was not counted.

Extraction name	Counter filling		Counter efficiency before rise time or energy cuts		Day counting began in 1995		Live time of counting (days)		Δ	
	GeH_4 Fraction (%)	Pressure (mm Hg)	*L* peak	*K* peak	*L* peak	*K* peak	*L* peak	*K* peak	*L* peak	*K* peak
Cr 1	6.5	690	0.335	0.356	5.82	2.90	137.8	142.1	0.618	0.734
Cr 2	8.0	685	0.326	0.344	10.42	10.35	134.5	136.7	0.753	0.767
Cr 3	7.5	650	0.329	0.338	19.41	19.34	104.0	105.6	0.792	0.804
Cr 4	8.5	665	0.329	0.341	35.39	35.32	132.3	134.8	0.824	0.837
Cr 4-2	13.5	650	—	0.321	—	37.24	—	126.6	—	0.584
Cr 5	7.5	650	0.350	0.359	61.52	61.52	119.6	122.0	0.760	0.774
Cr 6	8.7	645	0.359	0.365	84.44	84.38	120.7	123.4	0.506	0.521
Cr 6-2	13.5	695	—	0.350	—	86.21	—	152.0	—	0.841
Cr 7	7.0	645	0.329	0.337	114.49	114.29	129.8	132.4	0.775	0.784
Cr 8	7.0	700	0.324	0.347	145.41	145.41	151.8	154.9	0.729	0.747

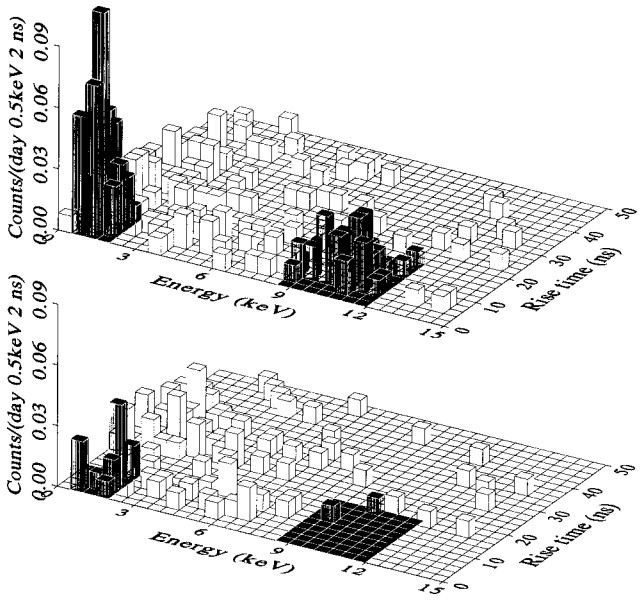

FIG. 11. Upper panel shows the energy rise time histogram of all events observed during the first 30 days after extraction for the first five Cr exposure measurements. The live time is 120.1 days. The expected location of the ^{71}Ge *L* and *K* peaks is shown darkened. Lower panel shows the same histogram for all events that occurred during an equal live time interval at the end of counting.

After the counting of the samples from the Cr experiment was completed, in the fall of 1995, measurements of the counting efficiency were made. Two different techniques and three different isotopes were employed: ^{37}Ar to measure volume efficiency, and ^{69}Ge and ^{71}Ge to measure the *L*- and *K*-peak efficiencies [36]. The volume efficiency of all counters used for first extractions was directly measured with ^{37}Ar. The calculated counting efficiency, using the measured pressure, GeH_4 fraction, and ^{37}Ar volume efficiency, is given for each extraction in Table IX. The total uncertainty in these calculated efficiencies is 3.1%.

VI. DATA ANALYSIS AND RESULTS

A. Event selection

Candidate ^{71}Ge events were selected in exactly the same manner as in our extractions to measure the solar neutrino capture rate. The first step was to apply time cuts to the data that serve to suppress false ^{71}Ge events that may be produced by Rn outside the proportional counter and by Rn added to the counter during filling. In the next step, events that were in coincidence with the surrounding NaI counter were eliminated. For the first five extractions, a histogram of the 250 events that remained which occurred during the first 30 days after extraction is given in the upper panel of Fig. 11. The darkened areas are the locations of the ^{71}Ge *L* and *K* peaks as predicted from the ^{55}Fe and ^{109}Cd calibrations. For comparison, an identical spectrum of the 113 events that occurred in these extractions during an interval of equal live time at the end of counting (more than 122 days after extraction) is given in the lower panel of Fig. 11. The ^{71}Ge *L* and *K* peaks are very obvious in the spectrum at the beginning of counting, but are absent in the spectrum at the end of counting because the ^{71}Ge has decayed away. The number of counts outside the two peaks is approximately the same in both spectra because they were produced by background processes.

Windows with 98% acceptance in energy [2 full width at half maximum (FWHM) width] and 95% acceptance in rise time (0–10 ns in the *L* peak and 0–18.4 ns in the *K* peak) were then set around the *L* and *K* peaks. All events inside these windows during the entire period of counting were considered as candidate ^{71}Ge events.

B. Maximum likelihood analysis

The time sequence of the candidate ^{71}Ge events was analyzed with a maximum likelihood method [37] to separate the ^{71}Ge 11.4-day decay from a constant rate background. The only differences between this analysis and that done for the solar neutrino runs are that one must account for the decay of the ^{51}Cr during the period of exposure, include a

TABLE X. Results of analysis of *L*-peak events selected by pulse shape. The production rate for the individual exposures is referred to the starting time of each exposure. The production rate for the combined result is referred to the time of the start of the first exposure. The second extractions were not counted in an electronics system with a digitizer so event selection based on pulse shape could not be made. The parameter Nw^2 measures the goodness of fit of the sequence of event times [45,46]. The probability was inferred from Nw^2 by simulation.

Extraction	Number of candidate events	Number fit to ^{71}Ge	Number of events assigned to			^{71}Ge Production rate by ^{51}Cr source (atoms/day)	Nw^2	Probability (percent)
			^{51}Cr source production	Solar ν production	Carryover			
Cr 1	23	20.9	22.5	0.4	0	$28.5^{+6.6}_{-6.8}$	0.173	24
Cr 2	22	11.9	10.4	0.3	1.1	$10.8^{+6.0}_{-2.9}$	0.036	81
Cr 3	22	11.9	11.4	0.5	0	$10.0^{+4.4}_{-3.5}$	0.062	43
Cr 4	24	15.1	13.8	0.6	0.7	$8.0^{+3.8}_{-1.8}$	0.082	37
Cr 5	20	8.8	7.9	0.9	0	$4.3^{+2.8}_{-1.7}$	0.079	31
Cr 6	34	0.6	0.0	0.5	0.2	$0.0^{+3.3}_{-0.0}$	0.045	82
Cr 7	14	2.9	2.1	0.8	0	$1.2^{+2.0}_{-0.7}$	0.118	23
Cr 8	11	2.8	2.2	0.7	0	$1.4^{+2.0}_{-1.1}$	0.067	50
Combined	170	78.2	71.6	4.7	1.9	$16.1^{+2.5}_{-2.3}$	0.104	25

TABLE XI. Results of analysis of *K*-peak events selected by pulse shape. See caption for Table X for further explanation.

Extraction	Number of candidate events	Number fit to ^{71}Ge	Number of events assigned to			^{71}Ge production rate by ^{51}Cr source (atoms/day)	Nw^2	Probability (percent)
			^{51}Cr source production	Solar ν production	Carryover			
Cr 1	20	16.4	15.9	0.5	0	$17.2^{+5.1}_{-4.7}$	0.035	90
Cr 2	18	12.2	10.6	0.4	1.2	$10.2^{+5.4}_{-2.9}$	0.319	3
Cr 3	18	13.2	12.7	0.5	0	$10.5^{+3.7}_{-2.8}$	0.515	1
Cr 4	12	10.4	9.1	0.6	0.7	$5.0^{+2.5}_{-1.4}$	0.060	69
Cr 5	15	7.9	6.9	0.9	0	$3.6^{+2.3}_{-1.2}$	0.034	84
Cr 6	8	2.8	2.1	0.5	0.2	$1.6^{+2.3}_{-1.0}$	0.041	79
Cr 7	12	1.0	0.1	0.9	0	$0.1^{+1.7}_{-0.1}$	0.071	60
Cr 8	10	2.0	1.2	0.7	0	$0.7^{+1.6}_{-0.5}$	0.064	59
Combined	113	67.5	60.3	5.1	2.1	$12.4^{+2.0}_{-1.8}$	0.042	87

fixed term for solar neutrino background, and add a carryover term arising from the ^{71}Ge that was not removed because of the approximately 15% inefficiency of the preceding chemical extraction.

The likelihood function ($\mathcal{L}$) for each extraction is given by Eq. (17) of Ref. [37],

$$\mathcal{L}=e^{-(bT_L+a\Delta/\lambda_{71})}\prod_{i=1}^{N}[b+ae^{-\lambda_{71}t_i}], \tag{3}$$

where b is the background rate, T_L is the live time of counting, λ_{71} is the ^{71}Ge decay constant, Δ is the probability that a ^{71}Ge atom that is extracted will decay during a time that it might be counted, and t_i are the times of occurrence of the N candidate events.

The parameter a contains contributions from the three separate processes (Cr source neutrinos, solar neutrinos, and carryover) that are able to give ^{71}Ge in each extraction, i.e., $a=a_{\mathrm{Cr}}+a_{\odot}+a_{\mathrm{carryover}}$. It follows from Eq. (11) and Eq. (12) of Ref. [37] that these three terms are given for extraction k by

$$a^k_{\mathrm{Cr}}=p_{\mathrm{Cr}}\epsilon^k\exp[-\lambda_{51}(t^k_s-T)] \times[\exp(-\lambda_{51}\theta^k_{\mathrm{Cr}})-\exp(-\lambda_{71}\theta^k_{\mathrm{Cr}})]/(1-\lambda_{51}\lambda_{71}), \tag{4}$$

$$a^k_{\odot}=p_{\odot}\epsilon^k[1-\exp(-\lambda_{71}\theta^k_{\odot})], \tag{5}$$

$$a^k_{\mathrm{carryover}}=a^{k-1}\frac{\epsilon^k}{\epsilon^{k-1}}\exp(-\lambda_{71}\theta^k_{\odot})[1-\epsilon^{k-1}_{\mathrm{Ga}}]. \tag{6}$$

Here p_{Cr} and $p_{\odot}$ are the rates of production of ^{71}Ge by the ^{51}Cr source and solar neutrinos, respectively; λ_{51} is the decay constant of ^{51}Cr; t_s is the starting time of each source exposure; T is the source activity reference time of 18:00 on 26 December 1994; θ_{Cr} and $\theta_{\odot}$ are the times of exposure of the Ga to the ^{51}Cr source and to solar neutrinos, respectively; ϵ is the product of extraction and counting efficiencies; and $(1-\epsilon_{\mathrm{Ga}})$ is the inefficiency of extraction of Ge from the Ga. With these definitions, as the source decays, the production rate p_{Cr} is automatically referred to time T.

TABLE XII. Results of combined analysis of *L*- and *K*-peak events selected by pulse shape. See caption for Table X for further explanation.

Extraction	Number of candidate events	Number fit to ^{71}Ge	Number of events assigned to			^{71}Ge production rate by ^{51}Cr source (atoms/day)	Nw^2	Probability (percent)
			^{51}Cr source production	Solar ν production	Carryover			
Cr1	43	36.9	36.0	0.9	0	$22.0^{+4.1}_{-3.8}$	0.121	35
Cr2	40	24.0	21.1	0.7	2.3	$10.5^{+3.2}_{-2.9}$	0.202	3
Cr3	40	25.2	24.2	1.0	0	$10.3^{+2.6}_{-2.3}$	0.120	15
Cr4	36	25.2	22.5	1.3	1.4	$6.4^{+1.7}_{-1.5}$	0.061	61
Cr5	35	16.4	14.6	1.8	0	$3.9^{+1.5}_{-1.3}$	0.034	84
Cr6	42	4.1	2.8	0.9	0.3	$1.2^{+1.5}_{-1.0}$	0.046	79
Cr7	26	3.9	2.2	1.7	0	$0.6^{+1.0}_{-0.6}$	0.081	43
Cr8	21	4.5	3.1	1.4	0	$0.9^{+1.1}_{-0.8}$	0.034	89
Combined	283	143.7	130.0	9.8	4.0	$14.0^{+1.5}_{-1.5}$	0.068	50

In the maximization procedure to obtain p_{Cr} for each run, the solar production rate $p_{\odot}$ was held fixed at 0.27/day, the rate corresponding to 69 SNU [2] on 13.1 tons of Ga. Since second extractions followed extractions 2, 4, 6, and 7, the carryover correction was only applied to extractions 2, 4, and 6. Errors on p_{Cr} with one sigma confidence were set by finding the values of the rate that decreased the likelihood function from its value at the maximum by the factor $e^{-0.5}$. For each test value of p_{Cr} during this search, all the variables in the likelihood function except p_{Cr} were maximized. The overall production rate from the Cr source $p_{\mathrm{Cr}}^{\mathrm{global}}$ was obtained by maximizing the product of the likelihood functions for each run. In these maximizations the background rates in the L and K peaks for each run were free parameters.

C. Results

The set of Tables X, XI, and XII gives the results of the data analysis for the L peak, K peak, and $K+L$ peaks. The result for the global production rate in the combined fit to the eight extractions is $16.1^{+2.5}_{-2.3}$/day in the L peak, $12.4^{+2.0}_{-1.8}$/day in the K peak, and $14.0^{+1.5}_{-1.5}$/day in the $K+L$ peaks. The uncertainties here are all statistical. Figure 12 shows the $K+L$ combined results for the eight exposures and extractions. In the final three extractions only a few counts were produced by the ^{51}Cr source; so these results for the global production rates were almost unchanged if only the first five extractions were used in the combined fit.

A fit permitting the ^{71}Ge half-life to vary gave 13.5 ± 2.0 days, compared with its known half-life of 11.4 days.

Our solar neutrino results in the past have been based on events selected by ADP. Table XIII gives the results of analysis of the Cr extractions using the ADP method. (Since the ADP method is not capable of effectively analyzing the L peak, only K-peak results can be presented.) The result of the global fit to the eight extractions is $11.2^{+1.8}_{-1.7}$/day, in good agreement with the K-peak result that used the waveform measurement of rise time to select events.

Extraction 1 had a slight counting anomaly. The waveform digitizer was inoperative for the first 2.6 days of counting and only ADP information was available. During this short time period the events selected by ADP in the K peak were used to supplement those chosen by waveform analysis and no selection of L-peak events was made.

As described above, four of the eight extractions were followed with a second extraction. Three of these (Cr 2-2, Cr 4-2, and Cr 6-2) were counted in a similar way to the primary extractions, and the results are given in Table XIII (Cr 2-2 is missing because the counter failed). Because of the limited number of data acquisition channels which included a digitizer, these extractions were counted in an electronic system that was only able to make the ADP measurement of pulse shape. The combined results of extractions Cr 4-2 and Cr 6-2 showed no ^{71}Ge production by the ^{51}Cr source, as expected.

VII. SYSTEMATIC EFFECTS IN THE MEASUREMENT OF THE PRODUCTION RATE

A. Uncertainty in overall efficiency

A summary of the various contributions to the overall systematic uncertainty is given in Table XIV. Most of these components are the same as for the solar neutrino extractions; so the values for the solar runs are also given in Table XIV for comparison. The overall efficiency is the product of three factors: the chemical extraction efficiency, the saturation factor, and the counting efficiency. The uncertainty in each of these efficiencies will now be considered.

The major components of the uncertainty in the chemical extraction efficiency were the amount of Ge carrier added, the measured amount of Ge carrier extracted, and the amount of residual Ge carrier remaining from previous extractions. The concentration of Ge in the Ga:Ge alloy that was added as carrier was measured by atomic absorption spectroscopy and isotope dilution spectroscopy. The resultant total uncertainty in the amount of carrier added was $\pm2.1\%$. There was a $\pm3.5\%$ uncertainty in the measurements of the amount of Ge that was extracted; this value was larger than for the solar runs because of the smaller number of extractions performed. There were also $\pm0.5\%$ uncertainties in the amount of Ga

TABLE XIII. Results of analysis of K-peak events selected by ADP. The second extraction results were not used in the combined fit.

Extraction	Number of candidate events	Number fit to ^{71}Ge	Number of events assigned to			^{71}Ge production rate by ^{51}Cr source (atoms/day)	Nw^2	Probability (percent)
			^{51}Cr source production	Solar ν production	Carryover			
Cr 1	16	16.0	15.5	0.5	0	$15.3^{+4.0}_{-4.0}$	0.038	94
Cr 2	15	10.8	9.3	0.4	1.2	$9.2^{+5.0}_{-2.6}$	0.235	6
Cr 3	16	12.9	12.4	0.5	0	$10.4^{+3.7}_{-2.8}$	0.466	2
Cr 4	9	9.0	7.7	0.6	0.7	$4.3^{+2.4}_{-1.0}$	0.055	84
Cr 4-2	7	0.2	0.1	0.1	0	$0.1^{+2.0}_{-0.1}$	0.219	12
Cr 5	13	5.6	4.7	0.9	0	$2.5^{+2.1}_{-1.0}$	0.027	93
Cr 6	6	1.8	1.2	0.5	0.2	$0.9^{+2.0}_{-0.8}$	0.034	91
Cr 6-2	5	0.1	0.0	0.1	0	$0^{+1.0}_{-0.0}$	0.086	50
Cr 7	8	1.9	1.0	0.9	0	$0.6^{+1.6}_{-0.4}$	0.038	85
Cr 8	11	1.8	1.1	0.7	0	$0.6^{+1.6}_{-0.5}$	0.062	60
Combined	94	61.7	54.7	5.0	2.0	$11.2^{+1.8}_{-1.7}$	0.039	89

TABLE XIV. Summary of the contributions to the systematic uncertainty in the measured neutrino capture rate. Unless otherwise stated, all uncertainties are symmetric. The total is taken to be the quadratic sum of the individual contributions. For comparison, many of the systematics for the solar neutrino extractions are also provided. (Some of the solar values depend critically on the particular data set considered and are thus missing.) The statistical uncertainty in the result of the Cr experiment is $^{+11.1}_{-10.5}$%.

	Uncertainty in percent	
Origin of uncertainty	for solar runs	for Cr runs
Chemical extraction efficiency		
Mass of added Ge carrier	2.1	2.1
Amount of Ge extracted	2.5	3.5
Carrier carryover	0.5	0.5
Mass of gallium	0.5	0.5
Chemical extraction subtotal	3.3	4.1
Saturation factor		
Exposure time	0.14	0
Lead time	0.8	0
Saturation factor subtotal	0.8	0
Counting efficiency		
Calculated efficiency		
Volume efficiency	0.5	0.5
Peak efficiency	2.5	2.5
Simulations to correct for counter filling	1.7	1.7
Calibration statistics		
Centroid	0.1	0.1
Resolution	0.3	0.3
Rise time cut	0.6	0.6
Gain variations	—	+2.0
Rise time window offset	—	0
Counting efficiency subtotal	+4.4,−3.2	+3.7,−3.1
Residual radon after time cuts	—	−1.7
Solar neutrino background	0	1.2
^{71}Ge carryover	0	0.3
Total systematic uncertainty	—	+5.7,−5.6

and the amount of residual Ge carrier. Adding these components in quadrature yields a total uncertainty in the chemical extraction efficiency of ±4.1%.

The saturation factor for the Cr source [for solar neutrinos] is defined as the factors that multiply $p_{\mathrm{Cr}}\epsilon^k[p_\odot\epsilon^k]$ on the right-hand side of Eq. (4) [Eq. (5)]. The time of exposure to the source θ_{Cr} depended only on when the source was inserted and removed from the Ga-containing reactor, and was very well established; so the uncertainty in the source saturation factor was negligible. There was a minor uncertainty in the time of solar exposure $\theta_\odot$ because the extraction was made from two reactors and the mean time of extraction was used as the end time of exposure. But since the production rate from solar neutrinos was much less than from the Cr source, the uncertainty in the solar saturation factor was also negligible.

The uncertainty in the calculated counting efficiency was mentioned in Sec. V. The three components are the uncertainty in volume efficiency (0.5%), in measurements to determine peak efficiency (2.5%), and in simulations used to correct for differing GeH_4 percentages and counter pressures (1.7%), giving a combined uncertainty of 3.1%. The uncertainty in counting also includes the statistical uncertainty arising from the limited number of events in the ^{55}Fe calibrations, which typically had 1000–5000 events each. There were ±0.1%, ±0.3%, and ±0.6% uncertainties in the counting efficiency due to the uncertainties in the extrapolated ^{71}Ge *L*- and *K*-peak centroid, resolution and rise time limits, respectively. Finally, there was a +2.0% uncertainty due to gain variations during the time that the ^{71}Ge was decaying. This value is one sided because gain drifts can only shift the ^{71}Ge peak out of the event selection window. Adding these uncertainties in quadrature gave a total uncertainty in the production rate of $^{+3.7}_{-3.1}$% due to the uncertainty in the counting efficiency.

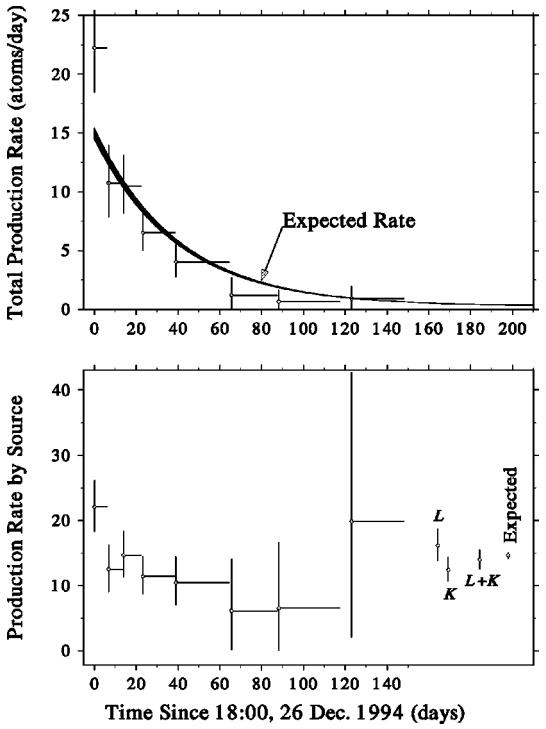

FIG. 12. The eight ^{71}Ge production rate measurements. The horizontal lines indicate the beginning and ending of each exposure with the vertical lines showing the measured production rate and its statistical error. The upper panel shows the total ^{71}Ge production rate from the source and from solar neutrinos. The expected rate calculated from the 517 kCi source activity and the cross section of Bahcall [38] is shown darkened. The lower panel shows only the production rate from the ^{51}Cr source, where each rate has been normalized to the time of the start of the first exposure. The combined results of all measurements are shown at the right, with the *L*-peak, *K*-peak, and *L*- plus *K*-peak results shown separately. The expected production rate and its uncertainty are shown at the extreme right.

B. Other systematic uncertainties

The final uncertainty that is common to both the Cr experiment and the solar neutrino measurements arises from the inefficiency of a 3.25-h time cut for Rn that might be added to the counter at the time it was filled. By analyzing the first five extractions both with and without this cut, we found that it removed a total of 22 events assigned to ^{71}Ge. Since the cut deletes all but 10% of false ^{71}Ge events, this implies that 2.2 false events may remain after the cut. As the total number of events assigned to ^{71}Ge in these five runs after the cut was 129.4, the systematic uncertainty after the cut was thus -1.7%. The value is negative since radon decays mistakenly identified as ^{71}Ge can only increase the observed signal.

Two systematic errors in Table XIV are unique to the Cr-source experiment. As discussed in Sec. VI B, there is an additional contribution to the measured signal from solar neutrinos and there is a carryover correction due to the incomplete removal of ^{71}Ge in the previous chemical extraction.

Although the production of ^{71}Ge in 13 tons of Ga by solar neutrinos is small, it is finite and a correction is necessary. We took the solar neutrino capture rate to be 69 SNU [2] and subtracted from the observed signal an amount corresponding to that production rate. The solar neutrino rate has been measured by SAGE to a precision of 12 SNU or 17%. However, the solar neutrino production was only a 6.8% correction (9.8 events out of 143.7) and thus its uncertainty resulted in a small (1.2%) uncertainty in the measured ^{51}Cr production rate.

The efficiency for extracting Ge from the Ga was typically 85%. Thus a fair amount of Ge remained in the Ga after extraction. Immediately following extractions for the solar neutrino runs, a second extraction is usually carried out. Because of these second extractions and because the time between extractions is several ^{71}Ge lifetimes, the number of Ge atoms that survive to the end of the next solar run is negligible. In the Cr experiment extraction schedule, however, this was not always the case. Second extractions were conducted only after extractions 2, 4, 6, and 7; so extractions 2, 4, and 6 contain a small contribution from ^{71}Ge produced during the previous exposure. The total number of events ascribed to ^{71}Ge was 143.7 with an uncertainty of approximately 10%. The total number of estimated carryover events was 4.0 which is determined with the same 10% uncertainty. Therefore the uncertainty in the ^{51}Cr production rate due to the uncertainty in the carryover correction was 0.3%.

VIII. MEASURED PRODUCTION RATE

The quadratic combination of all the systematic uncertainties described in the last section is $^{+5.7}_{-5.6}\%$. The measured production rate in the *K* and *L* peaks given in Sec. VI C, including both statistical and systematic errors, thus becomes $p_{\mathrm{Cr}}=14.0\pm1.5\ (\mathrm{stat})\pm0.8\ (\mathrm{syst})$ atoms of ^{71}Ge produced per day. This production rate is equivalent to about 3500 SNU, 50 times higher than the rate from solar neutrinos.

For comparison, in the GALLEX ^{51}Cr experiments [16], the average measured source production rate at the beginning of the first exposure was 11.1 ^{71}Ge atoms per day and the production rate from solar neutrinos and other background sources was 0.7/d. Even though our source had one-third the intensity of a GALLEX source, our production rate was nearly one-third higher and our background rate (see Sec. VI B) was a factor of 3 lower. This illustrates the significant advantage of using Ga metal with its high atomic density as the target for a neutrino source experiment. Further, our source had very high enrichment and consequent small physical size, leading to a long path length through the gallium absorber.

IX. MEASURED NEUTRINO CAPTURE CROSS SECTION

For a neutrino source of activity *A*, it follows from the definition of the cross section σ that the capture rate p of neutrinos in a material around the source can be written as the product

$$p=AD\langle L\rangle\sigma, \tag{7}$$

where $D=\rho N_0 f_I/M$ is the atomic density of the target isotope (see Table XV for the values and uncertainties of the constants that enter D), and $\langle L\rangle$ is the average neutrino path length through the absorbing material, which in the case of a homogeneous source that emits isotropically is given by

TABLE XV. Values and uncertainties of the terms that enter the calculation of the cross section. All uncertainties are symmetric.

Term	Value	Uncertainty	
		Magnitude	Percentage
Atomic density $D=\rho N_0 f_I/M$			
Ga density ρ (g Ga/cm^3) [47]	6.095	0.002	0.033
Avogadro's number N_0 (10^{23} atoms Ga/mol)	6.0220	negligible	negligible
^{71}Ga isotopic abundance f_I (atoms ^{71}Ga/100 atoms Ga) [48]	39.8921	0.0062	0.016
Ga molecular weight M (g Ga/mol) [48]	69.72307	0.00013	0.0002
Atomic density D (10^{22} atoms ^{71}Ga/cm^3)	2.1001	0.0008	0.037
Source activity at reference time A (10^{16} ^{51}Cr decays/s)	1.9114	0.0022	1.2
Capture rate p (^{71}Ge atoms produced/day) (uncertainties combined in quadrature.)	14.0	1.7	12.1
Path length in Ga $\langle L\rangle$ (cm)	72.6	0.2	0.28
Cross section σ [10^{-45} cm^2/(^{71}Ga atom ^{51}Cr decay)]	5.55	0.68	12.3

$$\langle L\rangle=\frac{1}{4\pi V_S}\int_{\text{absorber}} dV_A \int_{\text{source}} \frac{dV_S}{r_{SA}^2}. \tag{8}$$

In this last equation r_{SA} is the distance from point S in the source to point A in the absorber and the source and absorber volumes are V_S and V_A, respectively.

The Ga-containing reactor in which the ^{51}Cr source was placed was nearly cylindrical, with a dished bottom. Based on accurate measurements of the reactor shape, the path length $\langle L\rangle$ was determined by Monte Carlo integration over the source and absorber volumes to be 72.6 ± 0.2 cm. The accuracy of this integration was verified by checking its predictions for geometries that could be calculated analytically and by noting that the measured Ga mass contained in the reactor volume agreed with that predicted by the integration. The sensitivity of $\langle L\rangle$ to the reactor geometry, to the position of the source in the Ga, and to the spatial distribution of the source activity were all investigated by Monte Carlo integration, and the uncertainty given above includes these effects.

Substituting our measured values of p_{Cr} (Sec. VIII) and A (Sec. IV), and the constants D (Table XV) and $\langle L\rangle$ into Eq. (7), we obtain

$$\sigma=[5.55\pm0.60(\text{stat})\pm0.32(\text{syst})] \times 10^{-45}\frac{\text{cm}^2}{^{71}\text{Ga atom } ^{51}\text{Cr decay}}. \tag{9}$$

Because the half-life for the ^{71}Ge to ^{71}Ga decay is well known, the part of this cross section that is due to the transition to the ^{71}Ge ground state can be accurately calculated. The value given by Bahcall [38] is 5.53×10^{-45} cm^2. The portion of our experimentally determined cross section that can result from transitions to the two other states in ^{71}Ge which can be excited by ^{51}Cr neutrinos (at 175 keV and 500 keV above the ^{71}Ge ground state) is thus $(0.02\pm0.68)\times10^{-45}$ cm^2. Alternatively, as shown by Hata and Haxton [39], by taking the ratio of the measured cross section to the ground state cross section, our measurement restricts the weak interaction strengths BGT of these two levels according to

$$1+0.667\frac{\text{BGT(175 keV)}}{\text{BGT(g.s.)}} +0.218\frac{\text{BGT(500 keV)}}{\text{BGT(g.s.)}}=1.00\pm0.12, \tag{10}$$

where BGT(g.s.)$=0.087\pm0.001$ is the strength of the transition to the ^{71}Ge ground state.

X. DISCUSSION

The primary motivation for the ^{51}Cr source experiment was to determine if there is any unexpected problem in either the chemistry of extraction or the counting of ^{71}Ge, i.e., to see if there is some unknown systematic error in one or both of the efficiency factors in ϵ, the product of extraction and counting efficiencies. If some such systematic error were to exist, then the value of ϵ that we have used in the preceding will be in error by the factor E, defined as $E\equiv\epsilon_{\text{true}}/\epsilon_{\text{measured}}$. Since the cross section is inversely proportional to ϵ, this hypothetical error is equivalent to the cross section ratio, $E=\sigma_{\text{measured}}/\sigma_{\text{true}}$. An experimental value for E can be set from our measured cross section, Eq. (9), if one assumes that the true cross section is equivalent to the theoretically calculated cross section. Then $E\approx R\equiv\sigma_{\text{measured}}/\sigma_{\text{theoretical}}$. Neutrino capture cross sections averaged over the four neutrino lines of ^{51}Cr have been calculated by Bahcall [38] and by Haxton [40].

Bahcall, assuming that the strength of the two excited states in ^{71}Ge that can be reached by ^{51}Cr neutrinos is accurately determined by forward-angle (p,n) scattering, gives a result of 5.81 $(1.0^{+0.036}_{-0.028})\times10^{-45}$ cm^2. The upper limit for the uncertainty was set by assuming that the excited state strength could be in error by as much as a factor of 2; minor contributions to the uncertainty arise from forbidden corrections, the ^{71}Ge lifetime, and the threshold energy.

An independent consideration of the contribution of ex-

cited states has been made by Hata and Haxton [39] and very recently by Haxton [40]. They argue that, because of destructive interference between weak spin and strong spin-tensor amplitudes in ^{71}Ge, the strengths determined from (p,n) reactions are, for some nuclear levels, poor guides to the true weak interaction strength. In particular, Haxton finds the weak interaction strength of the $(5/2)^-$ level in ^{71}Ge at an excitation energy of 175 keV to be much greater than the value that is measured by the (p,n) scattering reaction, and calculates a total ^{51}Cr cross section of $(6.39\pm0.68)\times10^{-45}$ cm^2. This cross section was deduced from the measured (p,n) cross sections for the two excited states, and uses a large-basis shell model calculation to correct for the presence of spin-tensor contributions. Since not all known theoretical uncertainties were included, the stated error here is a lower bound.

Combining our statistical and systematic uncertainties for the cross section in quadrature into an experimental uncertainty, we can thus give estimates for E:

$$E\approx R\equiv\frac{\sigma_{\text{measured}}}{\sigma_{\text{theoretical}}}=\begin{cases}0.95\pm0.12(\text{expt})^{+0.035}_{-0.027}(\text{theor}) & (\text{Bahcall}),\\ 0.87\pm0.11(\text{expt})\pm0.09(\text{theor}) & (\text{Haxton}).\end{cases}\tag{11}$$

With either of these theoretical cross sections, R is consistent with unity, which implies that the total efficiency of the SAGE experiment to the neutrinos from ^{51}Cr is close to 100%.

The measurement reported here should not be interpreted as a direct calibration of the SAGE detector for solar neutrinos. This is because the ^{51}Cr neutrino spectrum differs from the solar spectrum, there is a 10%–15% uncertainty in the theoretical value for the ^{51}Cr cross section, and the total experimental efficiency for each solar neutrino measurement is known to a higher precision than the 12% experimental uncertainty obtained with the ^{51}Cr source. As a result, the solar neutrino measurements reported by SAGE should not be scaled by the factor E. Rather, we consider the Cr experiment as a test of the experimental procedures, and conclude that it has demonstrated *with neutrinos* that there is no unknown systematic uncertainty at the 10%–15% level.

The neutrino spectrum from ^{51}Cr is very similar to that of ^{7}Be, but at slightly lower energy. Since the response of ^{71}Ga to ^{7}Be neutrinos is governed by the same transitions that are involved in the ^{51}Cr source experiment, we can definitely claim that, if the interaction strength derived from the ^{51}Cr experiment is used in the analysis of the solar neutrino results, then the capture rate measured by SAGE includes the full contribution of neutrinos from ^{7}Be. This observation holds independent of the value of E or of cross section uncertainties. This demonstration is of considerable importance because a large suppression of the ^{7}Be neutrino flux from the sun is one consequence of the combined analysis of the four operating solar neutrino experiments [41,42].

GALLEX has completed two ^{51}Cr measurements whose combined result, using the cross section of Bahcall [38], can be expressed as $R=0.93\pm0.08$ [16], where the uncertainty in the theoretical cross section has been neglected. Both SAGE and GALLEX, which employ very different chemistries, give similar results for the solar neutrino capture rate and have tested their efficiencies with neutrino source experiments. The solar neutrino capture rate measured in Ga is in striking disagreement with standard solar model predictions and there is considerable evidence that this disagreement is not an experimental artifact.

ACKNOWLEDGMENTS

We thank E. N. Alexeyev, J. N. Bahcall, M. Baldo-Ceolin, L. B. Bezrukov, S. Brice, A. E. Chudakov, G. T. Garvey, W. Haxton, P. M. Ivanov, H. A. Kurdanov, V. A. Kuzmin, V. V. Kuzminov, V. A. Matveev, R. G. H. Robertson, V. A. Rubakov, L. D. Ryabev, and A. N. Tavkhelidze for stimulating our interest and for fruitful discussions. We acknowledge the support of the Russian Academy of Sciences, the Institute for Nuclear Research of the Russian Academy of Sciences, the Russian Ministry of Science and Technology, the Russian Foundation of Fundamental Research, the Division of Nuclear Physics of the U.S. Department of Energy, and the U.S. National Science Foundation. This research was made possible in part by Grant No. M7F000 from the International Science Foundation, Grant No. M7F300 from the International Science Foundation and the Russian Government, and Grant No. RP2-159 by the U.S. Civilian Research and Development Foundation.

[1] G. Audi and A. H. Wapstra, Nucl. Phys. **A595**, 409 (1995); A. H. Wapstra (private communication).
[2] J. N. Abdurashitov *et al.*, Phys. Lett. B **328**, 234 (1994).
[3] V. N. Gavrin, in Proceedings of the 18th International Conference on Neutrino Physics and Astrophysics, Takayama, Japan, 1998.
[4] J. N. Bahcall, M. Pinsonneault, and G. J. Wasserburg, Rev. Mod. Phys. **67**, 781 (1995).
[5] S. Turck-Chièze and I. Lopes, Astrophys. J. **408**, 347 (1993).
[6] W. Hampel *et al.*, Phys. Lett. B **388**, 384 (1996).
[7] B. T. Cleveland, T. J. Daily, R. Davis, Jr., J. R. Distel, K. Lande, C. K. Lee, and P. S. Wildenhain, Astrophys. J. **496**, 505 (1998).
[8] Y. Suzuki, Nucl. Phys. B (Proc. Suppl.) **38**, 54 (1995).
[9] J. N. Bahcall, Phys. Lett. B **338**, 276 (1994).
[10] V. Berezinsky, Comments Nucl. Part. Phys. **21**, 249 (1994).
[11] A. Parke, Phys. Rev. Lett. **74**, 839 (1995).
[12] N. Hata, S. Bludman, and P. Langacker, Phys. Rev. D **49**, 3622 (1994).
[13] V. Castellani, S. Degl'Innocenti, G. Fiorentini, M. Lissia, and B. Ricci, Phys. Rev. D **50**, 4749 (1994).
[14] J. N. Bahcall *et al.*, Nature (London) **375**, 29 (1995).
[15] K. M. Heeger and R. G. H. Robertson, Phys. Rev. Lett. **77**, 3720 (1996).
[16] W. Hampel *et al.*, Phys. Lett. B **420**, 114 (1998).
[17] J. N. Abdurashitov *et al.*, Phys. Rev. Lett. **77**, 4708 (1996).
[18] V. A. Kuzmin, Ph.D. thesis, Lebedev Physics Institute, Moscow, 1967, in Russian.

[19] L. W. Alvarez, Lawrence Radiation Laboratory, Physics Notes, Memo No. 767, 1973 (unpublished).
[20] R. S. Raghavan, in ''Proceedings of the Informal Conference on Status and Future of Solar Neutrino Research,'' Upton, New York, 1978, edited by G. Friedlander, Brookhaven National Laboratory Report No. 50879, Vol. 2, p. 270.
[21] W. C. Haxton, Phys. Rev. C **38**, 2474 (1988).
[22] *Table of Isotopes*, edited by V. S. Shirley, 8th ed. (Wiley, New York, 1996), p. 209.
[23] V. N. Gavrin, S. N. Danshin, G. T. Zatsepin, and A. V. Kopylov, Institute Nuclear Research Report No. P-335, 1984, in Russian.
[24] M. Cribier *et al.*, Nucl. Instrum. Methods Phys. Res. A **265**, 574 (1988).
[25] A. Tikhomirov, Nucl. Instrum. Methods Phys. Res. B **70**, 1 (1992).
[26] G. E. Popov *et al.*, Nucl. Instrum. Methods Phys. Res. A **362**, 532 (1995).
[27] A. V. Zvonarev *et al.*, At. Energy **80**, 107 (1996).
[28] V. N. Gavrin *et al*., in *Proceedings Inside the Sun Conference*, Versailles, France, 1989, edited by G. Berthomieu and M. Cribier (Kluwer, Dordrecht, 1989), p. 201.
[29] V. N. Gavrin *et al*., in *Proceedings Sixth International Workshop on Neutrino Telescopes*, Venice, Italy, 1994, edited by Milla Baldo Ceolin (Tipografia Franch, Piazzola, 1994), p. 199.
[30] I. N. Belousov *et al*., in *Proceedings of the International School on Particles and Cosmology*, Baksan Valley, Russia, 1991, edited by V. A. Matveev, E. N. Alexeyev, V. A. Rubakov, and I. I. Tkachev (World Scientific, Singapore, 1991), p. 59.
[31] C. Zhou, Nucl. Data Sheets **63**, 229 (1991).
[32] P. Anselmann *et al.*, Phys. Lett. B **342**, 440 (1995).
[33] U. Schötzig and H. Schrader, ''Halbwertszeiten und Photonenemissionswahrscheinlichkeiten von häufig verwendeten Radionukliden,'' Report No. PTB-Bericht PTB-Ra-16/4, Braunschweig, 1993.
[34] *Table of Radioactive Isotopes*, edited by V. S. Shirley (Wiley, New York, 1986).
[35] S. R. Elliott, Nucl. Instrum. Methods Phys. Res. A **290**, 158 (1990).
[36] J. N. Abdurashitov, A. O. Gusev, and V. E. Yants, in *Proceedings Eighth International School on Particles and Cosmology*, Baksan Valley, Russia, 1995, edited by E. N. Alexeyev, V. A. Matveev, Kh. S. Nirov, and V. A. Rubakov (World Scientific, Singapore, 1995), p. 70.
[37] B. T. Cleveland, Nucl. Instrum. Methods Phys. Res. **214**, 451 (1983).
[38] J. N. Bahcall, Phys. Rev. C **56**, 3391 (1997).
[39] N. Hata and W. Haxton, Phys. Lett. B **353**, 422 (1995).
[40] W. Haxton, Phys. Lett. B **431**, 110 (1998).
[41] S. A. Bludman, N. Hata, D. C. Kennedy, and P. G. Langacker, Phys. Rev. D **47**, 2220 (1993).
[42] E. Kh. Akhmedov, A. Lanza, and S. T. Petcov, Phys. Lett. B **348**, 124 (1995).
[43] *Handbook of Chemistry and Physics*, edited by D. P. Lide (CRC Press, Boca Raton, 1993).
[44] W. Heuer, Z. Phys. **194**, 224 (1966).
[45] A. W. Marshall, Ann. Math. Stat. **29**, 307 (1958).
[46] B. T. Cleveland, Nucl. Instrum. Methods Phys. Res. A **416**, 405 (1998).
[47] H. Köster, F. Hensel, and E. U. Franck, Ber. Bunsenges. Phys. Chem. **74**, 43 (1970).
[48] L. A. Machlan, J. W. Gramlich, L. J. Powell, and G. M. Lambert, J. Res. Natl. Bur. Stand. **91**, 323 (1986).